Three-peak evolution characteristics of supporting stress on a super-long working face in a thick coal seam

Hongbing Wang[1], Zhiheng Cheng[2]*, Jinhu Zhang[3,4,5]*, Liang Chen[2], Xin Luo[6,7], Meichen Li[2], Haoyi Chen[1] and Yifei Xie[2]

[1]School of Civil and Resource Engineering, University of Science and Technology Beijing, Beijing, China, [2]School of Mining Safety, North China Institute of Science and Technology, Beijing, China, [3]CCTEG Coal Mining Research Institute, Beijing, China, [4]Coal Mining and Designing Department, Tiandi Science and Technology Co., Ltd., Beijing, China, [5]School of Energy and Mining Engineering, China University of Mining Technology-Beijing, Beijing, China, [6]School of Emergency Management and Safety Engineering, China University of Mining Technology-Beijing, Beijing, China, [7]School of Emergency Technology and Management, North China Institute of Science and Technology, Langfang, China

Increasing working face length is the development trend of intelligent and efficient longwall fully mechanized mining. By combining field measurement and theoretical calculation, change characteristics of the frequency, peak value, and range of weighting in a long working face in a 1000 m-deep shaft of Kouzidong Coal Mine (Fuyang City, Anhui Province, China) were studied. Based on the mechanical model of the hydraulic support group of the elastic independent support, force characteristics and posture change characteristics of the support in the 121304 working face of the mine were studied and analyzed. The supporting stress characteristics of the deep super-long working face were revealed, and the theoretical calculation was in good agreement with the actual measurement. Based on the aforementioned model, support parameters and control technology of the 140502 working face were studied. The results show that as the length of the working face increases, the supporting stress gradually transforms from a single peak to multiple peaks and expands to both ends of the working face. The weighting in different areas of the working face is characterized by an obvious time sequence and great difference in intensity. When the working face length is 300 m, the multi-peak characteristic of super-long working faces appears. The M-shaped three-peak characteristic can be used as the criterion for super-long working faces. A reasonable working face length should be determined by comprehensively considering occurrence conditions of coal seams, working face parameter, and equipment ability. According to the different attributes of hydraulic supports in space and function and combining with zonal characteristics of the long working face, the criterion for the super-long working face and the principle of zonal cooperative control of hydraulic support groups were revealed. In addition, a cooperative control method of equipment groups in the working face based on the state error and cost functions was put forward, and the three-level cooperative control strategy and implementation method were formulated. It can effectively guide the equipment group in the super-long fully mechanized working face in deep thick coal seams to achieve optimal coordinated control.

1 Introduction

With the development of efficient coal mining technologies (Wu et al., 2022; Li et al., 2023a), the spatial scale of fully mechanized working faces in coal mines in China constantly expands in three aspects: mining depth, horizontal scale (including the working face length and advance length), and vertical scale (mainly the mining height) (Liu et al., 2021; Zou et al., 2022a; Ye et al., 2022; Li et al., 2023b; Ma et al., 2023; Sun et al., 2023). In such context, the mining depth of coal increases at a speed of 10–25 m/a, and the working face length gradually increases from 100–200 m to 300–350 m, and even above 400 m in some cases (Li et al., 2021; Zou et al., 2022b; Zhang et al., 2023a; Su et al., 2023; Ye et al., 2023). The increases in the burial depth and working face length cause significant changes in strata behaviors (Zhang et al., 2022a; Liang et al., 2022; Ran et al., 2023a), and more pre-existing cracks are found in surrounding rocks of deep mines (Ran et al., 2023b; Zhang et al., 2023b; Zou et al., 2023). As a result, the weighting in working faces occurs more frequently with a smaller step, in different areas (Wang et al., 2019; He et al., 2022; Liang et al., 2023). Some scholars found the decrease in the lumpiness of broken rocks in the key strata of overburden with the increase in working face length, accompanied by weighting of the main key strata, through similar material simulation and field measurement (Zuo et al., 2021; Gao et al., 2022; Liu et al., 2022). A high-intensity working face (characterized by the large mining height, long working face, and fast advance speed) was simplified into a two-dimensional (2D) beam model (He et al., 2020; Behera et al., 2021; Lou et al., 2021). The research found that the height–length ratio of broken rocks in the main roof increases due to the growing thickness of the load-bearing layer, mining height, and working face length. In addition, rock blocks in the main roof are highly prone to sliding during the first weighting, which is the cause for intense strata behaviors during shallowly buried high-intensity mining. Based on bearing characteristics of hydraulic supports (Ren et al., 2022; Zhang et al., 2022b), some researchers (Xu and Wang, 2017; Xu et al., 2018; Chi et al., 2021; Zhang et al., 2022b) built the rock beam model for hydraulic support groups of the elastic independent support, deduced the matrix equation for the supporting stress field of hydraulic supports for the roof, and offered the corresponding simplified calculation method. Some established the three-dimensional (3D) numerical model for a fracture zone in overlying strata of deep stopes with thin bedrocks and thick unconsolidated layers (Zhang et al., 2015), based on the pressure arch, stress shell, and Platts theories (Ma and Wu, 2021; Wang et al., 2022). Then, influences of the working face length on the height of the fracture zone and support resistance were quantitatively analyzed. Numerical analysis and field measurement were also conducted to reveal that load-bearing arches can be formed in overlying strata of shallowly buried longwall faces (Ren and Qi, 2011). In addition, the working face has a critical length. Once exceeding the critical length, it exerts lowered influences on the stability of overlying strata. An energy model (Mohammad et al., 2015) fully considering the geometry of stopes and mechanical parameters of rocks was built and compared with the results of field measurement, the theoretical model, and the numerical model,

revealing that the model is able to effectively predict the height of fracture zones in a stope. Previous research (Song and Wang, 2014; Wang and Ju, 2014) also found the W-shaped distribution characteristic of pressure in the dip direction of the working face by analyzing the strata behaviors in a 450 m super-long fully mechanized working face in Halagou Coal Mine (Shaanxi Province, China). Obviously, existing research on roof fracture along the length direction of working faces mainly summarized mine pressure using field measurements and analyzed its influencing factors combining numerical simulation (Chen et al., 2021; Zhao et al., 2021).

For further quantitative analysis, the research quantitatively analyzed the influencing factors of roof stability of a super-long working face buried about 1,000 m underground in Kouzidong Coal Mine (SDIC Xinji Energy Co., Ltd., Huainan, Anhui Province). Two working faces, 121304 and 140502, were observed, and mine pressure data were analyzed. On this basis, the distribution characteristics of supporting stress of hydraulic support groups and the weighting characteristics in the super-long fully mechanized working face in a deep thick coal seam were theoretically analyzed based on the model of the elastic independent support. In addition, the influencing factors of mine pressure in the super-long working face were revealed. According to distribution of the supporting stress in the super-long fully mechanized working face in the deep thick coal seam and combining the coupling characteristics of hydraulic supports and surrounding rocks, the principle, method, and control strategy of zonal cooperative control were proposed. The adaptability of hydraulic supports was improved through zonal cooperative control of hydraulic support groups in different areas, which provides a new method for roof control of intelligent working faces in similar coal mines.

2 Materials and methods

2.1 Overview of the deep super-long working face and model establishment

2.1.1 Overview of the coal mine

The coal seam of the 121304 working face in Kouzidong Coal Mine is buried 1,000 m underground and has a thickness of 2.2–6.7 m (5.18 m on average). The immediate roof of the working face is interbedding of mudstone and sandy mudstone with the thickness of 4.2–10.1 m and low hardness; the main roof is siliceous-cemented fine sandstone, with an average thickness of 5.0 m. The working face is 350 m long and excavated through full-seam mining with a large mining height. ZZ13000/27/60D four-leg shield hydraulic supports with a center-to-center distance of 1750 mm were used in the working face.

2.1.2 Model establishment

The supporting stress distribution of hydraulic support groups in the super-long working face can be analyzed using the elastic support model (Xu and Wang, 2017). As shown in Figure 1A (Xu et al., 2018), the model regards each support and the roadway walls

FIGURE 1
Model. **(A)** Hydraulic support groups regarded as an elastic support; **(B)** discrete single-span beam.

at both ends of the working face as elastomers of certain rigidity. Then, the relationship of the rigidity matrix $\{K\}$, moment of a single-span beam $\{M\}$, and load $\{Q\}$ of hydraulic supports is established based on the deformation compatibility condition of the rock beam (Xu and Wang, 2017).

As shown in Figure 1A a Cartesian system is established to analyze the stress field of the coal around a borehole: a linear pore elastic model and the coordinate transformation equation are used to convert the stress state distribution of the borehole in the natural spatial coordinate system to a stress model in x-, y-, and z-direction centered on the borehole to solve for the stress distribution around the borehole. The transformation equation is as follows:

$$\{K\}\{M\} = \{Q\}, \tag{1}$$

where K, M, and Q in are determined using the following equations:

$$K = \begin{bmatrix} a_{11} & a_{12} & a_{13} & & & & & 0 \\ a_{21} & a_{22} & a_{23} & a_{24} & & & & \\ a_{31} & a_{32} & a_{33} & a_{34} & a_{35} & & & \\ & a_{42} & a_{43} & a_{44} & a_{45} & a_{46} & & \\ & & \ddots & \ddots & \ddots & & & \\ & & & & a_{n-1n-3} & a_{n-1n-2} & a_{n-1n-1} & a_{n-1n} \\ 0 & & & & & a_{nn-2} & a_{nn-1} & a_{nn} \end{bmatrix},$$

$$M = \begin{bmatrix} M_1 \\ M_2 \\ M_3 \\ M_4 \\ \vdots \\ M_{n-1} \\ M_n \end{bmatrix}, Q = \begin{bmatrix} b_1 \\ b_2 \\ b_3 \\ b_4 \\ \vdots \\ b_{n+1} \\ b_{n+2} \end{bmatrix}, \tag{2}$$

where K is the symmetric matrix and the coefficient is $a_{ij} = a_{ji}$. If we convert Figure 1A into the discrete single-span beam in Figure 1B, values of the aforementioned parameters can be calculated. In the working face in the figure, n-2 hydraulic supports are erected, on which uniform load q is applied. The center-to-center distance of hydraulic

supports is B; K_1 and K_n separately represent the rigidity of roadway walls, and K_i is the rigidity of hydraulic supports ($i = 2, 3, \cdots, n-1$); $K_{\theta 1}$ and $K_{\theta 2}$ separately denote the rigidity of rock beams at both ends; M_i represents the bending moment at each elastic support; and v_i refers to the displacement of each support (Xu et al., 2018).

If the thickness of roof strata above the support does not change, the inertia moment of rock beams above the support is I, the bending moment at each support is M_i, and the subsidence of supports is v_i. The correlation coefficient of K and Q can be calculated according to Figure 1B (Zhang et al., 2022c).

$$\begin{cases} a_{11} = \dfrac{1}{K_{\theta 1}} + \dfrac{B}{3EI} + \dfrac{K_1 + K_2}{K_1 K_2 B^2} \\[2mm] a_{12} = \dfrac{B}{6EI} - \dfrac{1}{K_1 B^2} - \dfrac{2}{K_2 B^2} \\[2mm] a_{13} = \dfrac{1}{K_2 B^2} \\[2mm] a_{ii} = \dfrac{2B}{3EI} + \dfrac{1}{K_{i-1}B^2} + \dfrac{4}{K_i B^2} + \dfrac{1}{K_{i+1}B^2}, \\[2mm] a_{nn-2} = \dfrac{1}{K_{n-2}B^2} \\[2mm] a_{nn-1} = \dfrac{B}{6EI} - \dfrac{2}{K_{n-1}B^2} - \dfrac{1}{K_n B^2} \\[2mm] a_{nn} = \dfrac{1}{K_{\theta 2}} + \dfrac{B}{3EI} + \dfrac{K_{n-1} + K_n}{K_{n-1}K_n B^2} \end{cases} \tag{3}$$

$$\begin{cases} b_1 = \dfrac{qB^3}{24EI} - \dfrac{q}{2K_1} + \dfrac{q}{K_2} \\[2mm] b_2 = \dfrac{qB^3}{12EI} + \dfrac{q}{2K_1} - \dfrac{2q}{K_2} + \dfrac{q}{K_3} \\[2mm] b_i = \dfrac{qB^3}{12EI} + \dfrac{q}{K_{i-1}} - \dfrac{2q}{K_i} + \dfrac{q}{K_{i+1}} \\[2mm] b_{n-1} = \dfrac{qB^3}{12EI} + \dfrac{q}{K_{n-2}} - \dfrac{2q}{K_{n-1}} + \dfrac{q}{2K_n} \\[2mm] b_n = \dfrac{qB^3}{24EI} + \dfrac{q}{K_{n-1}} - \dfrac{q}{2K_n} \end{cases} \tag{4}$$

The model parameters include a mining height of 5.5 m, support rigidity of 0.48 GN/m, thickness of roof strata of 15 m, bulk density of rocks of 27 kN/m³, and elastic modulus of the roof of 40 GPa.

2.2 Conditions of the coal seam and determination method for supporting intensity in the working face

2.2.1 Conditions of the coal seam

The No. 5 coal seam, which has a simple structure and is mineable in the whole area, was mined in working face 140502. The average thickness of the coal seam is 6.56 m. The roof and floor are dominated by mudstone, with a small amount of fine sandstone, siltstone, and sandy mudstone. The immediate roof is composed of mudstone, with an average thickness of 2.81 m; the main roof consists of siltstone and sandstone, which are separately 7.65 and 13.85 m thick on average. The immediate floor mainly contains mudstone with an average thickness of 1.62 m. The main roof is interbedding of siltstone and sandstone and is 5.56 m thick on average. The dip angle of the coal seam is 8°–15° (14° on average), and the strike pitch in some areas of the working face is 17°.

2.2.2 Determination method of supporting intensity

The full-seam down-dip mining method was adopted in working face 140502, and the maximum mining height was 7 m. Because of the large burial depth, large mining height, and softness of the coal seam, reasonable selection of hydraulic supports is the key to safe and efficient mining of the working face. Considering the long-term usage in the Huainan Coal Mine area, four-leg shield hydraulic supports were adopted, which have been discussed in previous research (Wang et al., 2020), so it is not repeated here. The determination method for the reasonable supporting intensity required by the hydraulic supports was mainly introduced as follows. Previous research on the required supporting intensity in a working face buried 1,000 m underground in Tangkou Coal Mine (Xu et al., 2015) found that it is reasonable to use Eq. 5 to calculate the required supporting intensity of hydraulic supports in the deep working face.

$$P = (2.75 + \Psi)\frac{\gamma M}{K_P - 1}, \qquad (5)$$

where P, γ, K_p, M, and Ψ denote the supporting intensity, bulk density, bulking coefficient of rocks, mining height, and coupling factor, respectively. The equation adds coupling factor Ψ to the formula for estimating the supporting intensity of hydraulic supports based on the bulk density of rock pillars equivalent to the mining height. Coupling factor Ψ can be calculated as

$$\Psi = \frac{11l}{\beta 8} + \frac{11\sqrt[4]{\overline{\eta}\left(E_c + 2\beta^3 EIM\right)(\alpha + 2)\cos \alpha l}}{8E_c e^{\alpha l}}, \qquad (6)$$

where l, η, E_c, EI, and M represent the length of top beams, ratio of rigidity of hydraulic supports to that of coal, elastic modulus of coal

walls, flexural rigidity per unit width of rock beams in the roof, and mining height, respectively; $\alpha = \sqrt[4]{\frac{E_p}{4EIM}}$, and $\beta = \sqrt[4]{\frac{E_c}{4EIM}}$.

Obviously, coupling factor Ψ is a physical quantity related to the rigidity of hydraulic supports, lithology of the roof, and hardness of coal walls. If the supports and coal walls are regarded as rigid bodies, then $\Psi = 0$; that is, hydraulic supports are decoupled with surrounding rocks; if the supports and coal walls are elastomers, then $\Psi \neq 0$, which means that hydraulic supports are coupled with surrounding rocks. It is evident that Eq. 1 well describes the coupling relationship for the rigidity of hydraulic supports and surrounding rocks. The calculation parameters are set as follows (Pang et al., 2020): the elastic modulus of the coal seam is 30 GPa, the bulk density of rocks is 2.7 t/m³, the bulking coefficient is 1.35, the maximum mining height is 7 m, the top beam is 5 m long, and the hydraulic supports have a center-to-center distance of 1.75 m. According to the coupling formula for the rigidity of hydraulic supports and surrounding rocks, the curve of the required supporting intensity of hydraulic supports is attained, as shown in Figure 2.

The blue straight line in the figure represents that the required supporting intensity of hydraulic supports is calculated to be 1.48 MPa according to the weight of rock pillars equivalent to nine times the mining height. The black curve in the figure is the required supporting intensity of hydraulic supports obtained based on the coupling theory of the rigidity of hydraulic supports and surrounding rocks. Obviously, the required supporting intensity of hydraulic supports is closely related to the lithology of roof, thickness of coal seams, and rigidity of supports, and the calculation result obtained using the traditional method is lower. Because the rigidity of hydraulic supports is lower than that of the coal seam (Xu, 2015; Xu et al., 2019), the required supporting intensity of hydraulic supports should not be lower than 1.7 MPa. Therefore, the supporting intensity of the ZZ18000/33/72D four-leg shield hydraulic supports is determined to be in the range of 1.73–1.78 MPa.

Because the supporting stress of hydraulic supports increases and the strata behaviors in working faces are intensified as the mining height grows, determining a reasonable working face length is a focus for studying working face 140502. Compared with working face 121304, the maximum mining height of working face 140502 is as large as 7 m, and the main roof of the working face is thicker. The calculation parameters include the mining height (7 m), rigidity of supports (0.6 GN/m), thickness of roof strata (21 m), and bulk density of rocks (27 kN/m³).

3 Results and discussion

3.1 Characteristics of strata behaviors in the deep super-long working face

In the early mining period of the working face, a complete set of equipment including hydraulic supports was arranged in the working face and the roof was relatively stable. The overlying rock beam was interbedded in the strata and, therefore, can be regarded as rigidly fixed on the support (Figure 3). Under the condition, both the displacement and rotational angle at the
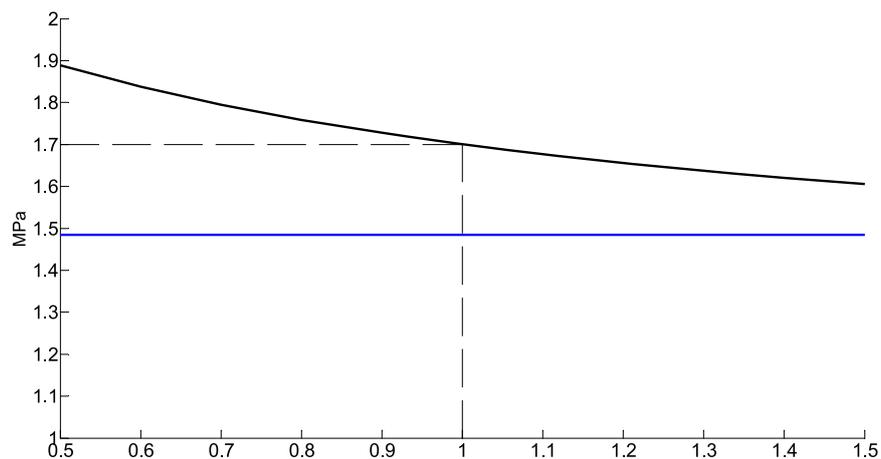
FIGURE 2
Required supporting intensity of hydraulic supports.
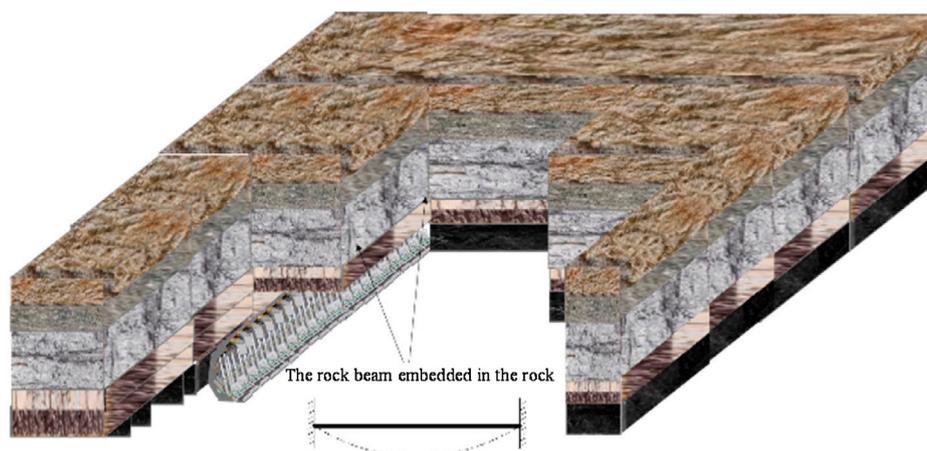
FIGURE 3
The roof is in a fixed support state after opening of the working face and at the initial stage of mining.

support were zero. Figures 4, 5 show the calculation results when considering roadway walls as rigid bodies (Figure 5 is the front view of the supporting stress of hydraulic support groups in the working face, that is, the projection of supporting stress in the working face onto the coal wall). It can be seen from the figures that the supporting stress has three peaks separately at points A, B, and C, which are located at 101 m, the middle, and 249 m of the working face, respectively. The supporting stress at points A and B is 1.3 MPa, and that at C is 1.26 MPa. Obviously, the peak values at points A and C are higher than that at B; that is, the peaks are high at both ends and low in the middle, forming a saddle shape seeming like the letter "M," so the phenomenon is collectively called three-peak M-like distribution.

To facilitate understanding of the distribution characteristics of the supporting stress of hydraulic support groups in the whole working face, the supporting force in Figure 4 is combined with the hydraulic support groups in the working face and data at each

coordinate in Figure 4 are displayed to a certain scale. In this way, distribution characteristics of supporting stress of hydraulic support groups in the working face on each hydraulic support are obtained.

After opening the coal seam in the working face, overlying strata have a space to fracture, cave, and rotate, so the rock beam has corresponding migration along both strike and dip directions of the working face. In this case, several support modes, including simple support, elastic support, and elastic fixed end displayed in Figures 6, 7, are present in the working face.

When regarding roadway walls as elastomers with the rigidity of 30 GN/m while keeping other calculation parameters unchanged, distribution characteristics of the supporting stress of hydraulic support groups are shown in Figures 8–10. It can be seen from Figure 9 that points A, B, and C are separately located at 77 m, the middle, and 273 m of the working face, respectively.
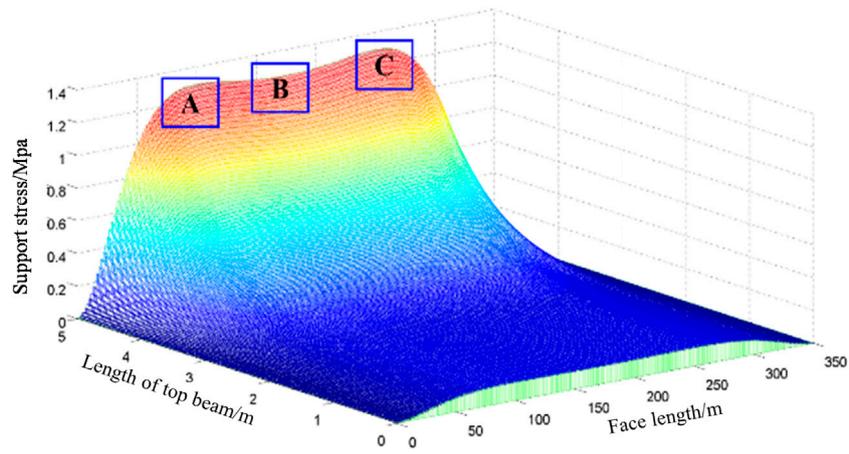
FIGURE 4
Supporting stress field of hydraulic supports.
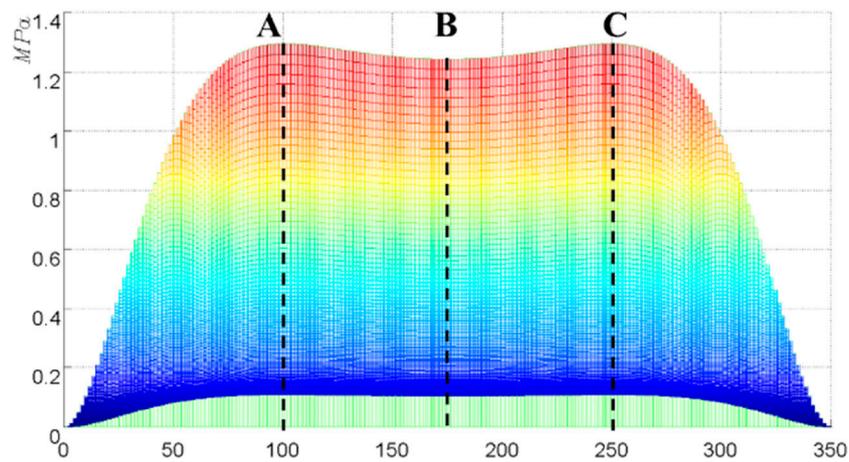
FIGURE 5
Front view of the supporting stress field.
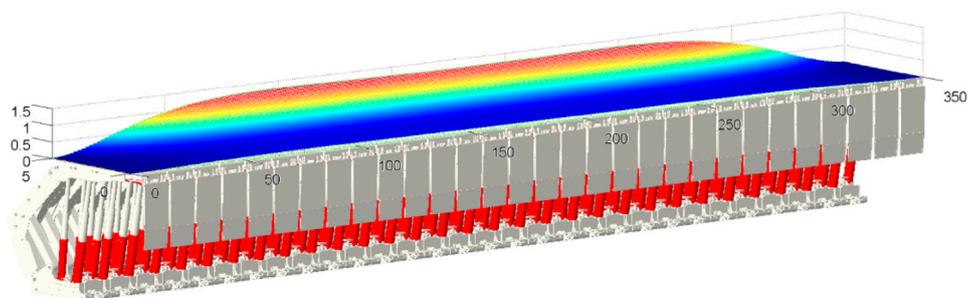
FIGURE 6
Supporting stress field of hydraulic support groups.
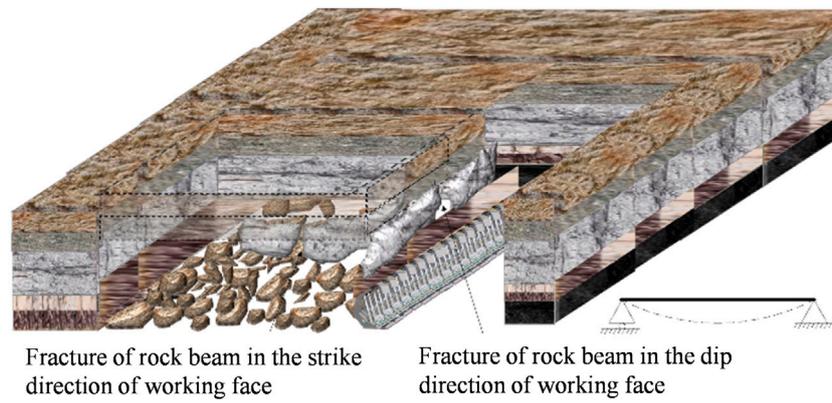
FIGURE 7
Roof collapse of the working face along the strike and dip directions in the normal mining stage.
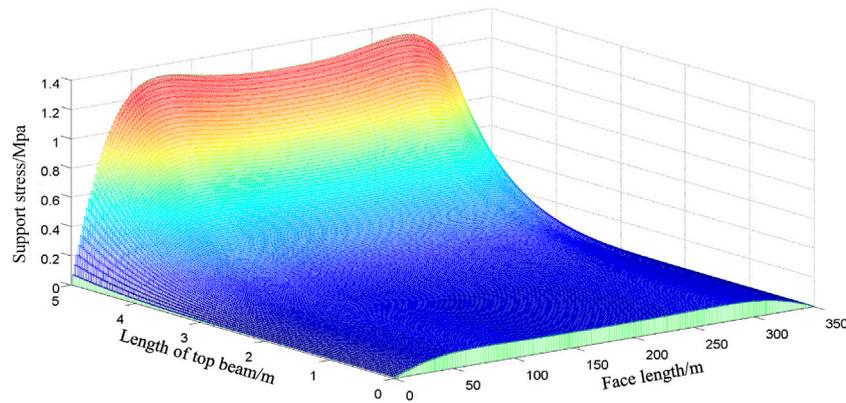
FIGURE 8
Supporting stress field of hydraulic supports.
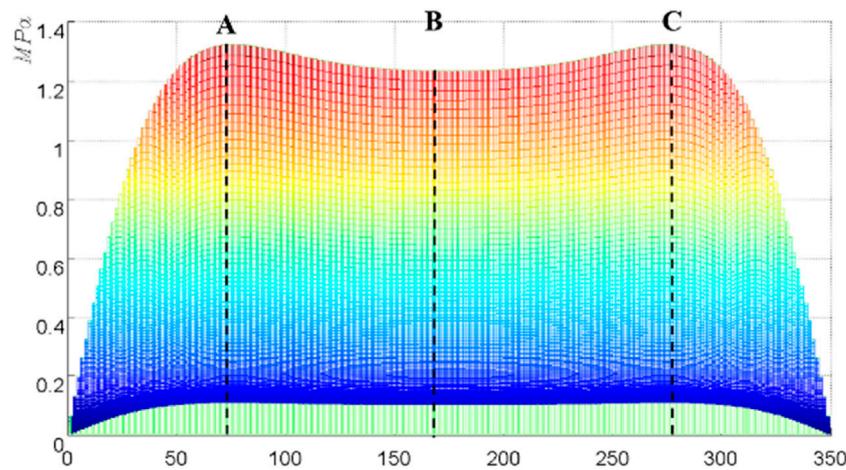
FIGURE 9
Front view of the supporting stress field.
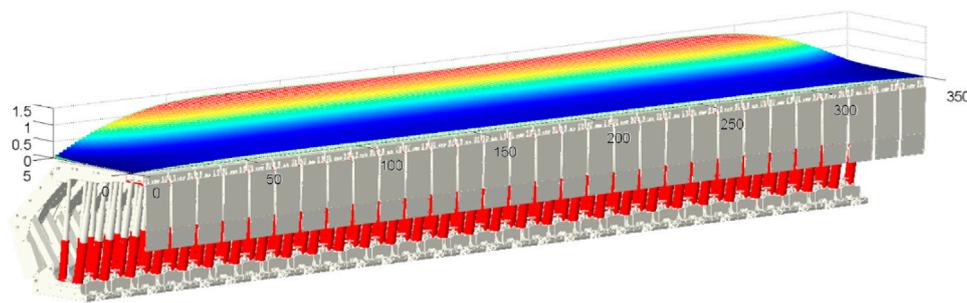
FIGURE 10
Distribution of the supporting stress of hydraulic support groups.

A comparison of Figures 5, 9 reveals that as the rigidity of roadway walls reduces, the maximum peak point A of the supporting stress shifts from the original location of 101 m–77 m in the working face; the maximum peak point B changes from the original location of 249 m–273 m; that is, the peak supporting stress of hydraulic supports shifts to both ends gradually and more supports in the working face are in the high-stress zones. Combined with Figures 3–10, the supporting stress of hydraulic supports in the super-long working face is distributed in a saddle shape with M-like three peaks, and large areas of hydraulic supports are in the high-stress zone.

3.2 Field-monitored support stress characteristics

The working resistance of hydraulic supports in working face 121304 was monitored online. Seven measuring lines were arranged separately along 9# and 189# supports on the upper and lower ends, 40# and 80# supports in the upper middle, 130# and 160# supports in the lower middle, and 100# support in the middle of the working face. Figure 11A shows the measured working resistance of hydraulic supports on the seven measuring lines along the advance direction of the working face; Figure 11B illustrates the measured values and distribution trends of working resistance of hydraulic supports on five profiles along the length direction of the working face under different advancing progresses. It can be seen from the figures that weighting in different areas of the working face shows obvious time sequences and different intensities, with a weighting step of 15–25 m and a smaller weighting step in the middle compared to the weighting step at both ends. Generally, weighting occurs first to the middle and lags behind in both ends of the working face. Particularly, the middle of the working face experiences weighting at a higher frequency with unobvious periodicity. Because the working face is long, the pressure on hydraulic supports in different areas varies significantly, showing a saddle-shaped distribution trend, which is in good agreement with the results of theoretical calculation.

Figures 12A–C separately show the supporting stress of hydraulic support groups when the working face length is 240, 300, and 350 m.

As shown in the figures, the supporting stress of hydraulic support groups begins to change from a single peak to multiple peaks with the increase in working face length. The supporting stress of hydraulic support groups has a single peak when the working face is 240 m long. The supporting stress begins to show the saddle-shaped three-peak M-like distribution when the working face length is 300 m. The saddle shape becomes more obvious when the working face is 350 m long, and the supporting stress begins to spread to both ends of the working face. It can be seen that the mining height exerts large influences on the distribution characteristics of the supporting stress of hydraulic support groups in the working face, so the working face length is determined to be 300 m.

3.3 Characteristics of the super-long working face in a deep thick coal seam

3.3.1 Relationship between the supporting stress and end conditions of the working face

Figure 13A shows the supporting stress of hydraulic support groups when changing roadway walls at two ends of the working face from rigid bodies to elastomers with a rigidity of 30 GN/m while keeping other conditions unchanged under the mining height and working face length separately of 7 and 240 m. The supporting stress of hydraulic support groups is distributed in the three-peak M-like pattern. Compared with Figure 12A, the supporting stress of hydraulic support groups begins to change from a single peak to three-peak M-like pattern as the rigidity of roadway walls at both ends of the working face reduces and more supports are located in the high-stress zone. It indicates that distribution of supporting stress in the working face is closely related to the condition of roadway walls at both ends. Obviously, the weaker the roadway walls are, the more likely it is for the supporting stress in the working face to show the three-peak M-like distribution under the same condition.

3.3.2 Relationship between the supporting stress in the working face and the lithology of the roof

Figure 13B shows the supporting stress of hydraulic support groups when the mining height and working face length are separately 7 and 300 m after adjusting the elastic modulus of the roof to 55 GPa while keeping other conditions unchanged. The

supporting stress only has a peak. Compared with Figure 12B, the supporting stress of hydraulic support groups begins to change from single-peak distribution to three-peak M-like distribution with the weakening of the roof, and more supports are located in the high-stress zone. The result suggests that the distribution of the supporting stress in the working face is closely related to the lithology of the overlying strata and roof. Obviously, the weaker the roof is, the more likely it is for the supporting stress in working face to show the three-peak M-like distribution under the same conditions.

3.3.3 Relationship between the supporting stress in the working face and the thickness of the main roof

Figure 13C displays the supporting stress of hydraulic support groups when the mining height is 7 m and working face length is 300 m after increasing the thickness of the main roof from 21 m to 30 m while keeping other conditions unchanged. As shown, the supporting stress of hydraulic support groups only has a peak. A comparison with Figure 12B reveals that as the thickness of the main roof decreases, the supporting stress of hydraulic support groups starts to turn from single-peak distribution to three-peak distribution and more
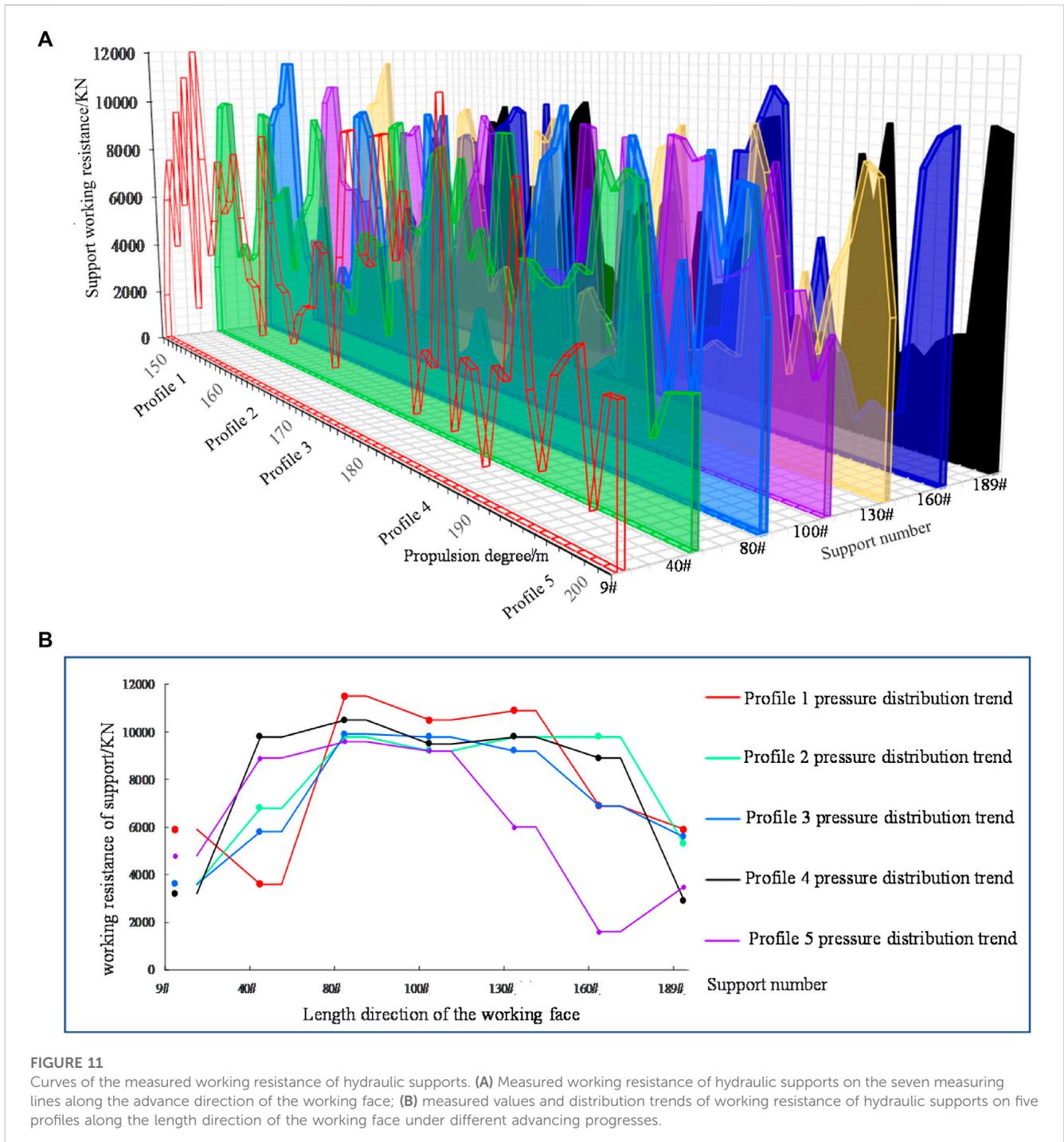
FIGURE 11
Curves of the measured working resistance of hydraulic supports. **(A)** Measured working resistance of hydraulic supports on the seven measuring lines along the advance direction of the working face; **(B)** measured values and distribution trends of working resistance of hydraulic supports on five profiles along the length direction of the working face under different advancing progresses.
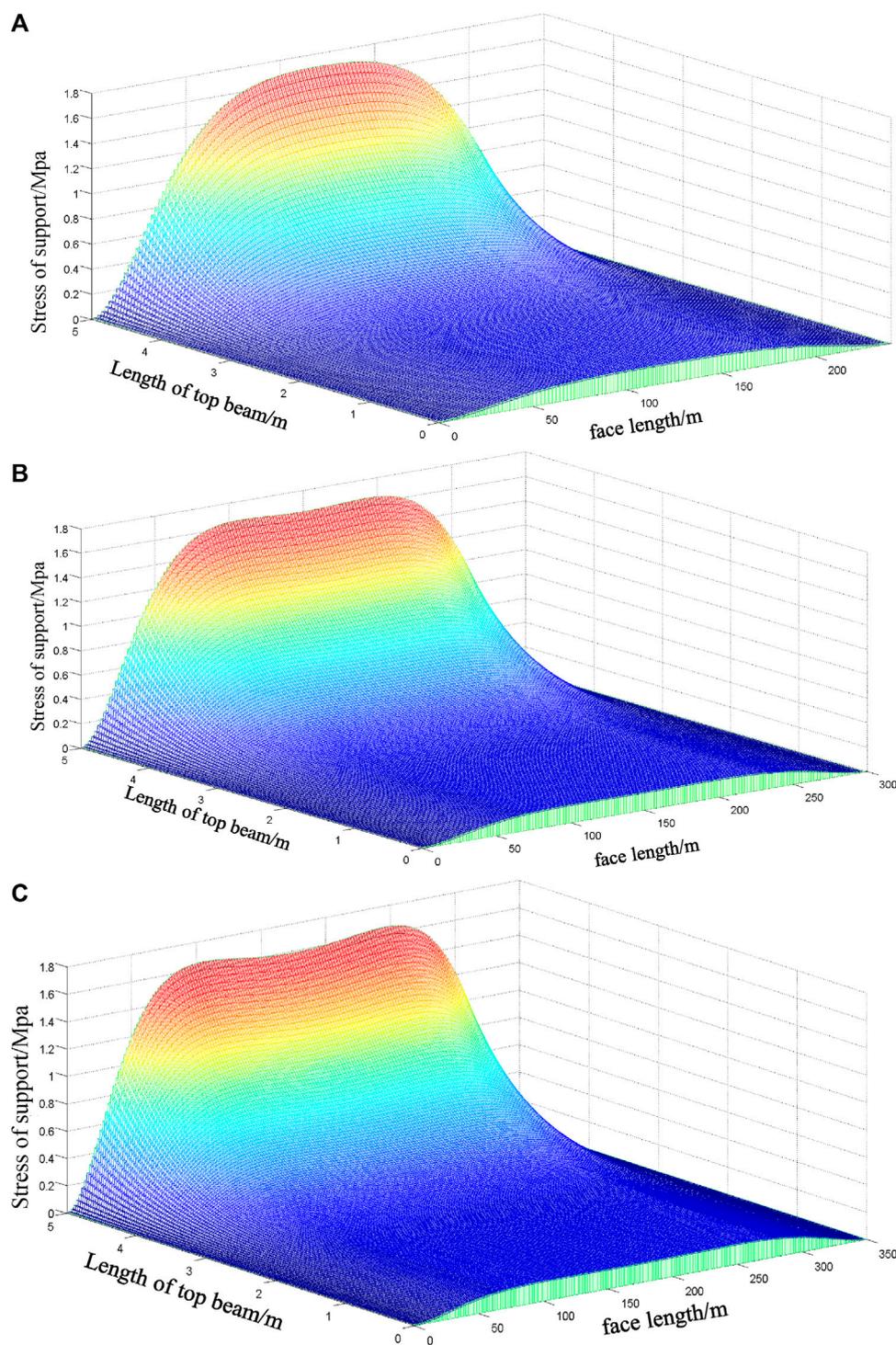
FIGURE 12
Supporting stress field of hydraulic support groups under different working face lengths. **(A)** The working face length is 240 m; **(B)** 300 m; **(C)** 350 m.

supports are found in the high-stress zone. The result indicates the close correlation between the distribution of the supporting stress in the working face and the thickness of the overlying bedrock. It is evident that the thinner the overlying bedrock is, the more likely it is for the supporting stress in the working face to show the three-peak M-like distribution under the same condition.

3.4 Criterion for the super-long working face

The presence of three-peak M-like distribution of the supporting stress in the working face is a characteristic first proposed in according to the measured pressure data in a 450 m super-long
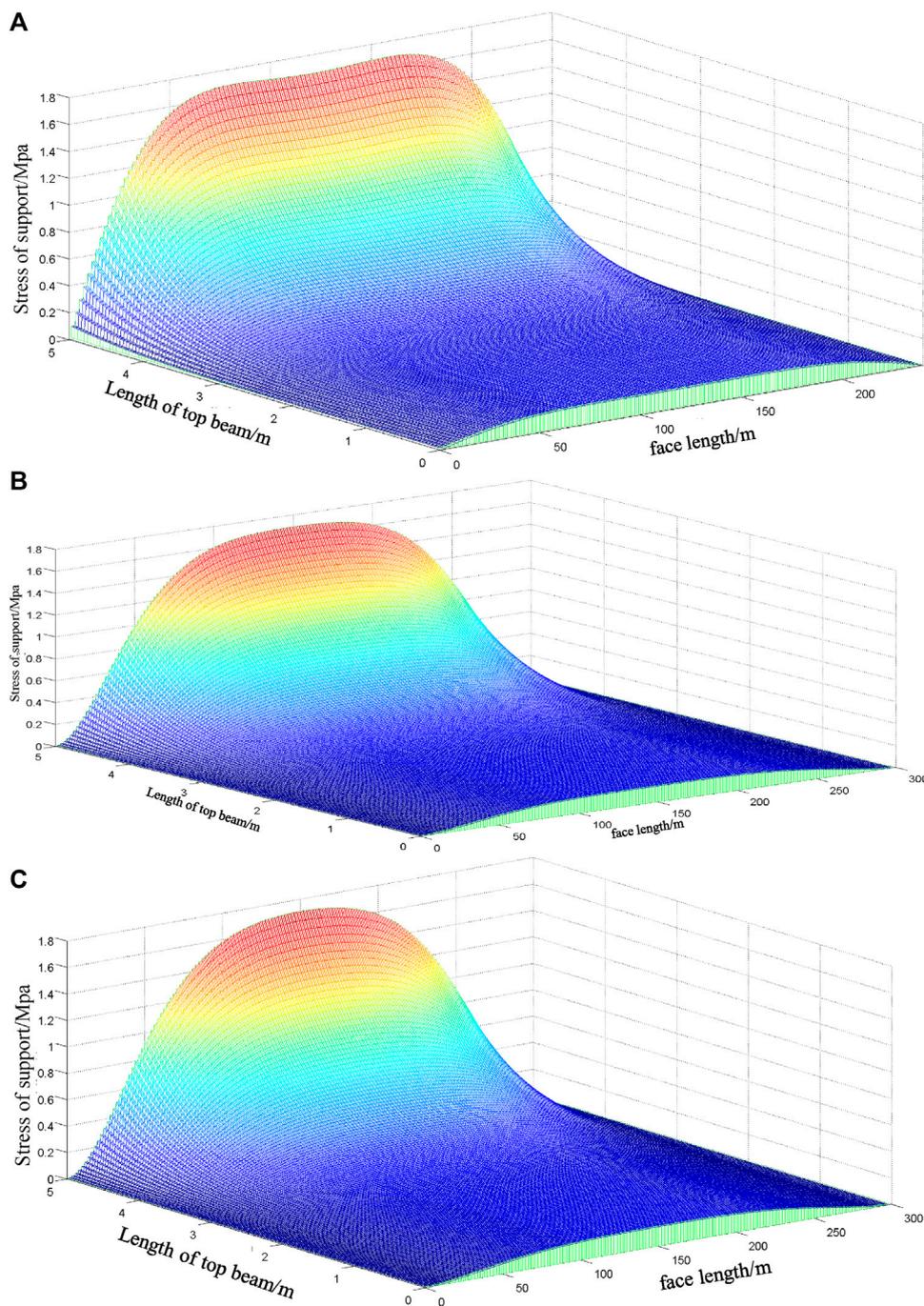
FIGURE 13
Supporting stress field of hydraulic supports. **(A)** The mining height and working face length separately of 7 and 240 m, bodies to elastomers with rigidity of 30 GN/m; **(B)** the mining height and working face length separately of 7 and 300 m, the elastic modulus of the roof to 55 GPa; **(C)** the mining height and working face length separately of 7 and 300 m, increasing the thickness of the main roof from 21 m to 30 m.

working face in Halagou Coal Mine (Song and Wang, 2014; Wang and Ju, 2014), which has also been studied in the work of Xu et al. (2018). According to the aforementioned analysis, the supporting stress of hydraulic support groups in the working face definitely turns from the single-peak distribution to three-peak M-like distribution with the increase in the working face length while keeping other conditions unchanged. After the occurrence of the

three-peak M-like distribution, the phenomenon becomes more significant once the working face length is further increased, and the peaks shift to both ends of the working face.

The three-peak M-like distribution of the supporting stress in the working face is closely related to the working face length and it is bound to occur once the working face length exceeds a certain value. This reveals that the three-peak M-like distribution characteristic is

an attribute specific for super-long working faces. Therefore, whether the supporting stress of hydraulic support groups in the working face has the three-peak M-like distribution characteristic or not can be taken as a criterion for super-long working faces.

The main cause for the three-peak M-like distribution of the supporting stress in the super-long working face was analyzed as follows. The aforementioned analysis indicates that under the same condition, as the support conditions of roadway walls at the ends of working faces weaken, the supporting stress in the working face begins to change from one peak to three peaks. This suggests that the support conditions of roadway walls at ends of the working face greatly influence the distribution pattern of the supporting stress in the working face. The influences of conditions of roadway walls at the ends on the supporting stress can be used to explain the cause for the three peaks of the supporting stress in the super-long working face. With the increase in working face length, the support action of the roadway walls at both ends of the working face for the overlying strata in the middle weakens. Under the same support conditions, the subsidence of overlying strata in the middle gradually increases so that more supports are located in the high-stress zone, and therefore, the supporting stress has three peaks. Once further increasing the working face length after the occurrence of the three-peak distribution of the supporting stress, the support action of roadway walls at both ends of the working face for the middle further weakens. The range in the middle of the working face where subsidence of overlying strata increases begins to expand to both ends and more supports are in the high-stress zone, which is shown as a shift of the peak supporting stress to both ends of the working face. Obviously, the supporting stress in the working face shows three peaks, which is caused by the weakened action of the support conditions at the ends on the overlying strata in the middle of the working face. This is the primary cause for the three-peak M-like distribution of the supporting stress in the super-long working face.

The three-peak M-like distribution of the supporting stress in the working face is not only determined by a single parameter (working face length) but also related to many conditions, including the burial depth, mining height, working face length, roof lithology, bedrock thickness, and condition of roadway walls. The three-peak M-like distribution occurs to the 450 m-long working face in Halagou Coal Mine; the distribution pattern appears in the 350 m-long working face in Kouzidong Coal Mine when the mining height is 5.5 m; and the distribution characteristic occurs in working face 140502 under the working face length of only 300 m when the mining height is 7 m. For the fully mechanized working face with a large mining height in deep thick coal seams, its length has to be determined reasonably according to the concrete occurrence conditions of the coal seams. Particularly for deep working faces of a large mining height, thin bedrock, soft coal seam, and fractured roof, the aforementioned aspects need to be fully considered to determine a reasonable working face length.

3.5 Cooperative control of equipment groups in the working face based on the state error and cost functions

As mentioned previously, the typical characteristic of the supporting stress in a super-long working face in a deep thick coal seam is the occurrence of three-peak M-like distribution. The

supporting stress of hydraulic supports varies across areas and its peak shits to both ends of the working face, and more hydraulic supports are located in the high-stress zone as the working face length increases. Because the roof pressure is large in the areas of the M-like three peaks, overlying strata in these areas are first fractured, followed by fracture of overlying strata at both ends bearing lower pressure. Roof weighting occurs first to the middle and then both ends of the working face, which is shown as asynchronized and frequent weighting in different areas of the working face. The three-peak M-like distribution of the supporting stress in the super-long working face well explains phenomena including weighting in different areas, frequent weighting, and multiple pressure peaks in working face 121304 of Kouzidong Coal Mine.

Aiming at the aforementioned phenomena, the key to improving the support capacity and adaptability of hydraulic supports in the super-long fully mechanized working face in the deep thick coal seam is to use the zonal cooperative control method; that is, different control strategies are used for hydraulic supports in different areas.

Due to changes in the distribution characteristics of stress in surrounding rocks of the super-long working face, hydraulic supports cannot be controlled using the consistent process parameters in their support and advance process. Otherwise, the consistent and continuous control of surrounding rocks and advance of equipment in the working face cannot be ensured. Therefore, how to automatically adjust mining parameters in different areas of the super-long working face to reach the optimal overall support effect and the highest advance efficiency has become a key problem to be solved. Here, a cooperative control method for equipment groups in the working face based on the state error and cost functions was proposed to realize the optimal coordinated control of equipment groups in the super-long fully mechanized working face in the deep thick coal seam.

As shown in Figure 14, the cooperative control method for equipment groups in the working face based on the state error and cost functions was established to realize the expected behaviors of equipment groups. These include four objectives for equipment groups: velocity consistency, desired trajectory and velocity tracking, aggregation, and collision avoidance. The state error is defined as follows:

$$\dot{\hat{X}} = A\hat{X} + B\hat{U}, \qquad (7)$$

where X, A, U, and B represent the aggregation stage of all objects in a system at a certain time, the state matrix, the control input of the system, and the control matrix, respectively.

The group problem is converted to an optimal control problem of aggregation containing three components of cost functions.

$$\begin{aligned} \min : J &= J_1 + J_2 + J_3, \\ s.t. \dot{\hat{X}} &= A\hat{X} + BU, \end{aligned} \qquad (8)$$

where J_1 is the cost function to ensure velocity consistency; J_2 is the cost function to ensure desired trajectory and velocity tracking, aggregation, and collision avoidance; and J_3 is the cost function of the cost control.

3.5.1 Control of hydraulic support groups

The control system of hydraulic support groups deduces specific parameters of three-peak M-like distribution of supporting stress in the super-long working face based on the
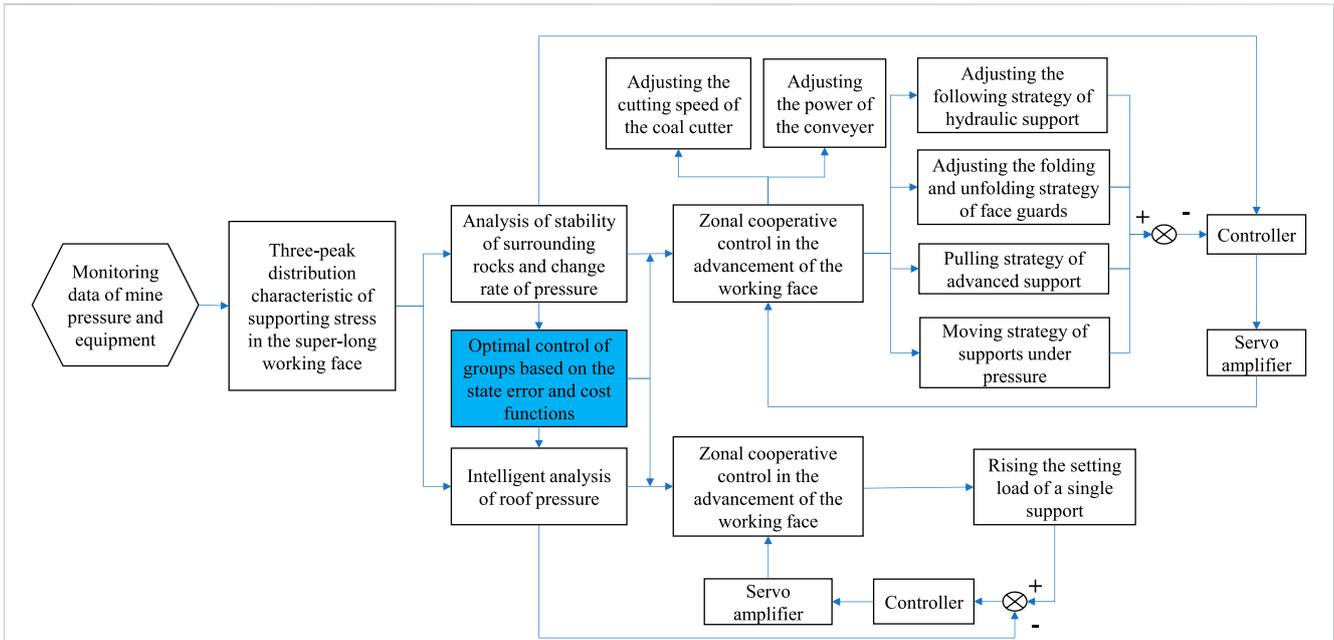
FIGURE 14
Method of group cooperative control of the working face.
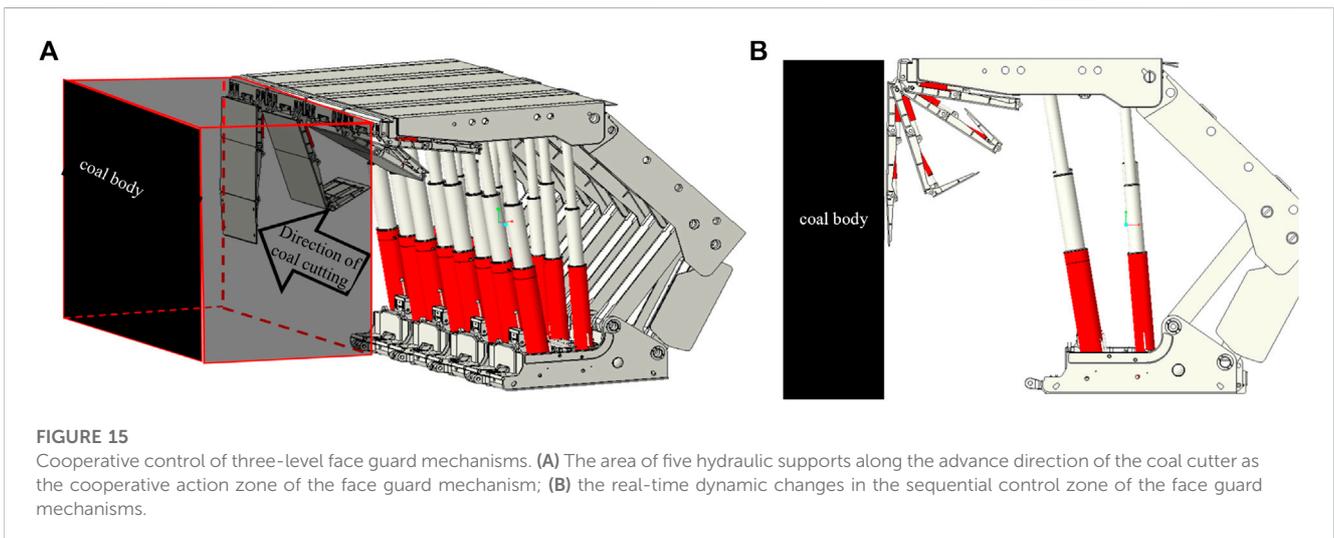
FIGURE 15
Cooperative control of three-level face guard mechanisms. **(A)** The area of five hydraulic supports along the advance direction of the coal cutter as the cooperative action zone of the face guard mechanism; **(B)** the real-time dynamic changes in the sequential control zone of the face guard mechanisms.

monitoring data of mine pressure and equipment. These parameters include the peak pressure, change rate, change period, maximum subsidence, and subsidence rate, which are separately input in control equation 8. In this way, the optimization model for the zonal adaptive control of supports and the zonal cooperative control of advancement of equipment for the working face is established. The adaptive control of supports means adaptive adjustment of the setting load of a single support; the cooperative control of advancement of equipment mainly refers to coordinated control of the hydraulic support, coal cutter, and scraper conveyer in areas of different pressures. The method is described in detail as follows: different control strategies are adopted in different

areas according to pressure distribution characteristics in the working face; then, the three-level cooperative control strategy of "single-support control → multi-support control → group control" is used; the information acquisition module is used to acquire information including the advancing progress of the working face, roof weighting step, weighting frequency, shrinkage of support, pressure on props, and dip angle of the roof for decision making; the hydraulic support group is controlled to support the roadway actively to realize zonal cooperative control of the supporting intensity, rigidity, and stability of supports (Kang et al., 2018).

Based on perceptual information including the pressure, dip angle, and pushing of a single support, the 3D posture of the single

support is controlled along the vertical, horizontal, and strike directions using strategies including support in the vertical direction, collapse resistance in the horizontal direction, and pushing control in the strike direction. The posture of the single support is automatically controlled via precise support in the vertical direction, quantitative pushing in the strike direction, and prevention of deviation in the horizontal direction using a series of cooperative control methods. These methods include roof support, protection of roadway walls, pushing, bottom lifting, lateral pushing, and balance. Because down-dip mining was adopted in the working face, the setting load guarantee system was used for real-time monitoring and increasing the setting load of hydraulic supports during down-dip mining, as shown in Figure 14, to avoid difficulty in caving of the suspended roof in the overlying strata. This can realize the immediate caving and unloading of the roof after mining and avoids gas accumulation in the goaf, which is detrimental to production safety.

According to zonal roof caving of the working face and the sequential relationship of cooperative advancement, hydraulic support groups at the head, middle, and tail of the coal cutter were controlled separately based on control demands for the strength, rigidity, and stability and combining with the geological and production conditions in different areas. The middle of the working face is characterized by the high peak pressure, high probability to bear impact loads, and large proportion of opened safety valves. Considering this, the strength and rigidity adaptability of hydraulic support groups in the middle should be mainly improved. The pressure rises rapidly on hydraulic support groups in some areas on two sides of the middle, where the strata behaviors are more intense than in the conventional working face and the support bears offset loads. Therefore, the strength and rigidity adaptability of the hydraulic supports should be improved on the premise of ensuring the stability. At both ends of the working face, especially the head of the coal cutter, the cooperative advance relationship of the hydraulic support groups with the advanced support system is mainly coordinated, and the location relationship of the two should be controlled with particular attention.

The zonal weighting determines that the equipment is inevitably advanced asynchronized in the advancement of the working face. After several mining cycles, the pressure on the equipment in the working face is not uniform, so the group control strategy should be used; that is, the hydraulic support groups in the working face are taken as the research object to automatically align the working face using a straightening system of working faces, so as to manage the hydraulic support groups.

3.5.2 Control of ends of the working face and roadway walls

As mentioned previously, the stability of ends of the working face and the roadway walls has some influences on the distribution of the supporting stress of hydraulic support groups in the working face. Because the roadway roof is fractured in Kouzidong Coal Mine, the supports at the ends of working faces and roadway walls should be enhanced, so as to improve the support capacity and adaptability of hydraulic supports in the whole working face. At first, high-strength anchor cables, high-strength bolts, and anchor meshes were

used for active high-strength support at the ends of the working face to improve stability of strata around the roadway. Then, high-strength face-end supports of high working resistance were adopted. On one hand, supports at the ends of the working face were stabilized, and on the other hand, the roof-cutting capacity of the face-end support was improved. Together with the automatic anchor withdrawal device, the pressure was relieved immediately at the ends of the working face. This avoids gas accumulation in the goaf and prevents the case that overlying strata of the roadway cannot cave and relieve pressure immediately after mining due to the high-strength support of roadway walls, otherwise causing gas accumulation in the goaf. Gas accumulation is very harmful for safe mining in the Huainan Coal Mine area of high gas content. The working face can be safely mined using the aforementioned method.

3.5.3 Cooperative control of protection of roadway walls

Most hydraulic supports in the middle of the working face are in a state of high supporting stress. According to the coupling of hydraulic supports and surrounding rocks, the coal wall is also under high pressure and, therefore, is prone to rib spalling. Because the maximum mining height is as large as 7 m, a three-level face guard mechanism was designed to realize the stable protection of coal walls. To ensure the cutting speed of the coal cutter and pushing of hydraulic supports in the working face, the area of five hydraulic supports along the advance direction of the coal cutter was determined as the cooperative action zone of the face guard mechanism. As shown in Figure 15A, the fifth support in front of the coal cutter for normal coal cutting needs to self-inspect the hydraulic system and move the extensible canopy before action, due to the sequential control in the cooperative action zone of the face guard mechanism of hydraulic supports. The fourth support in front of the coal cutter begins to move its face guard. The third-level face guard mechanism is withdrawn and folded, and the second- and first-level face guard mechanisms act simultaneously and the whole mechanisms are withdrawn to 25% of the completely withdrawal state. At the moment, the face guard mechanisms of the third and second hydraulic supports in front of the coal cutter have been withdrawn to 50% and 75% of the complete withdrawal state, while that of the first support that is adjacent to the coal cutter has been completely withdrawn. Under the condition, the face guard will not be cut when cutting coal to the first hydraulic support. The aforementioned process is repeated, and Figure 15B shows the real-time dynamic changes in the sequential control zone of the face guard mechanisms. Similar to this, after cutting coal using the coal cutter, the face guard mechanisms of hydraulic supports were unfolded, which act and support the coal wall, and hydraulic supports behind the coal cutter extend their extensible canopies and unfold their face guards successively. The automatic withdrawal and extension of face guards and extensible canopies in front of and behind the coal cutter, on one hand, prevent the cutting drum of the coal cutter from colliding and interfering with support beams, and on the other hand, this also achieves cooperative control of the action of hydraulic supports and the coal cutter, ensures stable control of coal walls and reliable support at the ends of working faces, and improves the efficiency of cooperative advancement of the coal cutter, scraper conveyer, and hydraulic supports in the working face.

4 Conclusion

The force characteristics and posture change characteristics of the support in the working face of the mine were studied and analyzed. The supporting stress characteristics of the deep super-long working face were revealed. Based on the aforementioned model, the support parameters and control technology of the working face were studied. The conclusions are shown as follows:

1) The studied working face in Kouzidong Coal Mine is a typical super-long working face in a deep thick coal seam. Strata behaviors in the working face show characteristics including an unobvious periodicity of weighting, an obvious time sequence, and greatly different intensities of weighting in different areas and the presence of many areas of peak pressure in the working face.

2) The presence of the three-peak M-like distribution of the supporting stress in the working face can be used as the criterion for a super-long working face. The three-peak distribution of the supporting stress in the super-long working face is a result of the weakened support action of support conditions in the roadway for the middle of the working face.

3) The three-peak M-like distribution of the supporting stress in the super-long working face is not only determined by a single parameter (working face length) but also related to many factors, including the burial depth, mining height, working face length, roof lithology, bedrock thickness, and condition of roadway walls. Therefore, the reasonable working face length should be determined according to the occurrence condition of the working face and coal seams in practical mining.

4) The zonal cooperative control for hydraulic support groups based on the state error and cost functions was used in the super-long deep working face, that is, the three-level cooperative control strategy of "single-support control → multi-support control → group control." The single-support control, multi-support control, and group control are an effective way to achieving safe and efficient support of super-long working faces in deep thick coal seams.

Data availability statement

Publicly available datasets were analyzed in this study. All data used during this research are available from the corresponding authors on reasonable request.

Author contributions

Conceptualization: ZC and JZ; methodology: HW; data curation: LC, ML, and HC; writing—original draft preparation: and HW and ZC; writing—review and editing: JZ, XL, and YX. All authors contributed to the article and approved the submitted version.

Funding

Conflict of interest

Author JZ was employed by Tiandi Science and Technology Co., Ltd.

The remaining authors declare that the research was conducted in the absence of any commercial or financial relationships that could be construed as a potential conflict of interest.

Publisher's note

References

Behera, B., Yadav, A., Singh, G. S. P., and Sharma, S. K. (2021). Assessment of excavation damage and spalling potential at a mechanized longwall face A numerical modeling study. *Geomechanics Geophys. Geo-Energy Geo-Resources* 7 (4), 104. doi:10.1007/s40948-021-00299-6

Chen, J. C., Zhou, L., Xia, B. W., Su, X. P., and Shen, Z. H. (2021). Numerical investigation of 3D distribution of mining-induced fractures in response to longwall mining. *Nat. Resour. Res.* 30 (1), 889–916. doi:10.1007/s11053-020-09759-4

Chi, X. L., Yang, K., and Wei, Z. (2021). Breaking and mining-induced stress evolution of overlying strata in the working face of a steeply dipping coal seam. *Int. J. Coal Sci. Technol.* 8 (4), 614–625. doi:10.1007/s40789-020-00392-3

Gao, Y. N., Lan, D. H., Zhang, Y. D., Chang, X. Y., Xie, J., and Gao, M. Z. (2022). The strata movement and ground pressure under disturbances from extra thick coal seam mining A case study of a coal mine in China. *Geomechanics Geophys. Geo-Energy Geo-Resources* 8 (6), 199. doi:10.1007/s40948-022-00506-y

He, M. C., Sui, Q. R., Li, M. N., Wang, Z. J., and Tao, Z. G. (2022). Compensation excavation method control for large deformation disaster of mountain soft rock tunnel. *Int. J. Min. Sci. Technol.* 32 (5), 951–963. doi:10.1016/j.ijmst.2022.08.004

He, Z. Q., Xie, H. P., Gao, M. Z., Deng, G. D., Peng, G. Y., and Li, C. (2020). The fracturing models of hard roofs and spatiotemporal law of mining-induced stress in a top coal caving face with an extra-thick coal seam. *Geomechanics Geophys. Geo-Energy Geo-Resources* 7 (1), 2. doi:10.1007/s40948-020-00202-9

Kang, H. P., Wang, G. F., Jiang, P. F., Wang, J. C., Zhang, N., Jing, H. W., et al. (2018). Conception for strata control and intelligent mining technology in deep coal mines with depth more than 1 000 m. *J. China Coal Soc.* 43 (7), 1789–1800. doi:10.13225/j.cnki.jccs.2018.0634

Li, B., Yang, X., Yuan, Y., Liang, Y. P., Li, S. Q., Zhu, C. Q., et al. (2023a). Experimental research on the influence of different factors on the behaviour of broken coal and rock particles during compaction. *Constr. Build. Mater.* 367, 130127. doi:10.1016/j.conbuildmat.2022.130127

Li, X. L., Zhang, X. Y., Shen, W. L., Zeng, Q. D., Chen, P., Qin, Q. Z., et al. (2023b). Research on the mechanism and control technology of coal wall sloughing in the ultra-large mining height working face. *Int. J. Env. Res. Pub He* 20 (2), 868. doi:10.3390/ijerph20010868

Li, X. L., Chen, S. J., Wang, S., Zhao, M., and Liu, H. (2021). Study on in situ stress distribution law of the deep mine Taking linyi mining area as an example. *Adv. Mater. Sci. Eng.* 2021, 5594181–5594211. doi:10.1155/2021/5594181

Liang, Y. P., Kong, F. J., Zou, Q. L., and Zhang, B. C. (2023). Effect of strain rate on mechanical response and failure characteristics of horizontal bedded coal under quasi-

static loading. *Geomechanics Geophys. Geo-Energy Geo-Resources* 9 (1), 52. doi:10.1007/s40948-023-00587-3

Liang, Y. P., Ran, Q. C., Zou, Q. L., Zhang, B. C., and Hong, Y. (2022). Experimental study of mechanical behaviors and failure characteristics of coal under true triaxial cyclic loading and unloading and stress rotation. *Nat. Resour. Res.* 31 (2), 971–991. doi:10.1007/s11053-022-10022-1

Liu, B. G., Song, Y., and Chu, Z. F. (2022). Time-dependent safety of lining structures of circular tunnels in weak rock strata. *Int. J. Min. Sci. Technol.* 32 (2), 323–334. doi:10.1016/j.ijmst.2021.12.003

Liu, T., Lin, B. Q., Fu, X. H., Zhao, Y., Gao, Y. B., and Yang, W. (2021). Modeling coupled gas flow and geomechanics process in stimulated coal seam by hydraulic flushing. *Int. J. Rock Mech. Min. Sci.* 142, 104769. doi:10.1016/j.ijrmms.2021.104769

Lou, J. F., Gao, F. Q., Yang, J. H., Ren, Y. F., Li, J. Z., Wang, X. Q., et al. (2021). Characteristics of evolution of mining-induced stress field in the longwall panel Insights from physical modeling. *Int. J. Coal Sci. Technol.* 8 (5), 938–955. doi:10.1007/s40789-020-00390-5

Ma, K., and Wu, J. (2021). Analytical study on limit support pressure of working face in underground space exploitation based on improved 3D wedge-prism model. *Geomechanics Geophys. Geo-Energy Geo-Resources* 7 (1), 10. doi:10.1007/s40948-020-00204-7

Ma, T. F., Liu, H. H., Zou, Q. L., Kong, F. J., Ran, Q. C., and Wang, P. T. (2023). Damage evolution characteristics and deterioration mechanism of mechanical properties of sandstone subjected to drying-wetting cycles. *J. Mater. Res. Technol.* 23, 4591–4605. doi:10.1016/j.jmrt.2023.02.068

Mohammad, R., Mohammad, F. H., and Abbas, M. (2015). A time-independent energy model to determine the height of de-stressed zone above the mined panel in longwall coal mining. *Tunn. Undergr. Space Technol.* 47, 81–92. doi:10.1016/j.tust.2015.01.001

Pang, Y. H., Wang, G. F., and Li, B. B. (2020). Stress path effect and instability process analysis of overlying strata in deep stopes. *J. Rock Mech. Eng.* 39 (4), 682–694. doi:10.13722/j.cnki.jrme.2019.0622

Ran, Q. C., Liang, Y. P., Zou, Q. L., Hong, Y., Zhang, B. C., Liu, H., et al. (2023a). Experimental investigation on mechanical characteristics of red sandstone under graded cyclic loading and its inspirations for stability of overlying strata. *Geomechanics Geophys. Geo-Energy Geo-Resources* 9 (1), 11. doi:10.1007/s40948-023-00555-x

Ran, Q. C., Liang, Y. P., Zou, Q. L., Zhang, B. C., Li, R. F., Chen, Z. H., et al. (2023b). Characteristics of mining-induced fractures under inclined coal seam group multiple mining and implications for gas migration. *Nat. Resour. Res.* 32 (3), 1481–1501. doi:10.1007/s11053-023-10199-z

Ren, P. F., Wang, Q., Tang, D. Z., Xu, H., and Chen, S. D. (2022). *In situ* stress-coal structure relationship and its influence on hydraulic fracturing A case study in zhengzhuang area in qinshui basin, China. *Nat. Resour. Res.* 31 (3), 1621–1646. doi:10.1007/s11053-022-10036-9

Ren, Y. F., and Qi, Q. X. (2011). Study on characteristic of stress field in surrounding rocks of shallow coalface under long wall mining. *J. China Coal Soc.* 36 (10), 1612–1618. doi:10.13225/j.cnki.jccs.2011.10.022

Song, L. B., and Wang, Q. X. (2014). Study on safety technology of China first 450 m ultra long fully mechanized coal face. *Coal Eng.* 46 (3), 45–51.

Su, E. L., Liang, Y. P., Chen, X. J., Wang, Z. F., Ni, X. M., Zou, Q. L., et al. (2023). Relationship between pore structure and mechanical properties of bituminous coal under sub-critical and super-critical CO2 treatment. *Energy* 280, 128155. doi:10.1016/j.energy.2023.128155

Sun, X. Y., Ran, Q. C., Liu, H., Ning, Y. H., and Ma, T. F. (2023). Characteristics of stress-displacement-fracture multi-field evolution around gas extraction borehole. *Energies* 16 (6), 2896. doi:10.3390/en16062896

Wang, G. F., Hu, X. P., Liu, X. H., Yu, X., Liu, W. C., Lv, Y., et al. (2020). Adaptability analysis of four-leg hydraulic support for underhand working face with large mining height of kilometer deep mine. *J. China Coal Soc.* 45 (3), 865–875. doi:10.13225/j.cnki.jccs.SJ19.1516

Wang, G. C., Yang, S. L., Yang, B. G., Li, Y., Wang, Z. H., Yang, Y., et al. (2019). Roof sub-regional fracturing and support resistance distribution in deep longwall face with ultra-large length. *J. China Coal Soc.* 44 (1), 54–63. doi:10.13225/j.cnki.jccs.2018.5139

Wang, Q., Wang, Y., He, M. C., Li, S. C., Jiang, Z. H., Jiang, B., et al. (2022). Experimental study on the mechanism of pressure releasing control in deep coal mine roadways located in faulted zone. *Geomechanics Geophys. Geo-Energy Geo-Resources* 8 (2), 50. doi:10.1007/s40948-021-00337-3

Wang, Q. X., and Ju, J. F. (2014). Study on mine strata pressure behavior of 450 m ultra long fully-mechanized coal mining face. *Coal Sci. Technol.* 42 (3), 125–128. doi:10.13199/j.cnki.cst.2014.03.033

Wu, Q. F., Yu, M. G., and Zheng, K. (2022). Experimental investigation on the effect of obstacle position on the explosion behaviors of the non-uniform methane/air mixture. *Fuel* 320, 123989. doi:10.1016/j.fuel.2022.123989

Xu, G. (2015). Experimental and theoretical study on hydraulic support in working face and its relationship with roof subsidence. *J. China Coal Soc.* 40 (7), 1485–1490. doi:10.13225/j.cnki.jccs.2015.0220

Xu, Y. J., Li, D. Y., Liu, X. K., and Ma, D. Z. (2019). Theoretical analysis and testing of vertical stiffness of hydraulic support. *Coal Min. Technol.* 24 (1), 40–44+52. doi:10.13532/j.cnki.cn11-3677/td.2019.01.009

Xu, Y. J., Wang, G. F., and Ren, H. W. (2015). Theory of coupling relationship between surrounding rocks and powered sup-port. *J. China Coal Soc.* 40 (11), 2528–2533. doi:10.13225/j.cnki.jccs.2015.7023

Xu, Y. J., and Wang, G. F. (2017). Supporting principle and bearing characteristics of hydraulic powered roof support groups. *Chin. J. Rock Mech. Eng.* 36 (S1), 3367–3373. doi:10.13722/j.cnki.jrme.2016.0706

Xu, Y. J., Wang, G. F., Zhang, J. H., Ren, H. W., and Li, D. Y. (2018). Theory and application of supporting stress fields of hydraulic powered support groups in fully mechanized mining face with large mining height based on elastic supporting beam model. *Chin. J. Rock Mech. Eng.* 37 (5), 1226–1236. doi:10.13722/j.cnki.jrme.2017.1471

Ye, C. F., Xie, H. P., Wu, F., and Li, C. B. (2022). Nonlinear creep properties and time-to-failure prediction of sandstone under saturated and dry conditions. *Environ. Earth Sci.* 81, 545. doi:10.1007/s12665-022-10666-5

Ye, C. F., Xie, H. P., Wu, F., and Li, C. B. (2023). Study on the nonlinear time-dependent deformation characteristics and viscoelastic-plastic model of shale under direct shear loading path. *Bull. Eng. Geol. Environ.* 82 (5), 189. doi:10.1007/s10064-023-03170-y

Zhang, B. C., Liang, Y. P., Zhao, Z. Y., Zou, Q. L., Zheng, H. L., Ning, Y. H., et al. (2023a). Effect of stress amplitude on mechanical and acoustic emission of sandstone under constant–cyclic loading. *Bull. Eng. Geol. Environ.* 82, 284. doi:10.1007/s10064-023-03307-z

Zhang, B. C., Liang, Y. P., Zou, Q. L., Ding, L. Q., and Ran, Q. C. (2023b). Experimental investigation into the damage evolution of sandstone under decreasing-amplitude stress rates and its implications for coalbed methane exploitation. *Environ. Earth Sci.* 82, 208. doi:10.1007/s12665-023-10825-2

Zhang, D. P., Yan, J., and Zhao, Y. Z. (2022c). Comparative study on development of ship structural mechanics in China and Russia. *Mech. Electr. Eng. Technol.* 51 (12), 43–46+60.

Zhang, T. C., Zou, Q. L., Jia, X. Q., Liu, T., Jiang, Z. B., Tian, S. X., et al. (2022a). Effect of cyclic water injection on the wettability of coal with different SiO2 nanofluid treatment time. *Fuel* 312, 122922. doi:10.1016/j.fuel.2021.122922

Zhang, T., Yuan, L., Zhao, Y. X., and Hao, X. J. (2015). Distribution law of working face pressure under the fracture zone distri-bution characteristic of deep mining. *J. China Coal Soc.* 40 (10), 2260–2268. doi:10.13225/j.cnki.jccs.2015.6006

Zhang, Y., Hou, S. H., Mei, S. H., Zhao, T. J., and Li, D. Y. (2022b). Experimental study of permeability-hydraulic fracturing characteristics of tight rocks. *Geomechanics Geophys. Geo-Energy Geo-Resources* 8 (6), 182. doi:10.1007/s40948-022-00499-8

Zhao, T., Gong, P. L., Yetilmezsoy, K., Bahramian, M., and Liu, C. Y. (2021). Dynamic failure and stability model analysis of thick and hard rock with wedge-structure immediate roof occurrence. *Geomechanics Geophys. Geo-Energy Geo-Resources* 7 (3), 80. doi:10.1007/s40948-021-00277-y

Zou, Q. L., Chen, Z. H., Cheng, Z. H., Liang, Y. P., Xu, W. J., Wen, P. R., et al. (2022a). Evaluation and intelligent deployment of coal and coalbed methane coupling coordinated exploitation based on Bayesian network and cuckoo search. *Int. J. Min. Sci. Technol.* 32 (6), 1315–1328. doi:10.1016/j.ijmst.2022.11.002

Zou, Q. L., Huo, Z. X., Zhang, T. C., Jiang, C. Z., and Liang, J. Y. (2023). Surface deposition characteristics of water-based SiO2 nanofluids on coal. *Fuel* 340, 127489. doi:10.1016/j.fuel.2023.127489

Zou, Q. L., Zhang, T. C., Ma, T. F., Tian, S. X., Jia, X. Q., and Jiang, Z. B. (2022b). Effect of water-based SiO2 nanofluid on surface wettability of raw coal. *Energy* 254, 124228. doi:10.1016/j.energy.2022.124228

Zuo, J. P., Yu, M. L., Li, C. Y., Sun, Y. J., Hu, S. Y., and Li, Z. D. (2021). Analysis of surface cracking and fracture behavior of a single thick main roof based on similar model experiments in Western Coal Mine, China. *Nat. Resour. Res.* 30 (1), 657–680. doi:10.1007/s11053-020-09735-y